

---

---

ISSN 1027-5495. Functional Materials, 25, No.3 (2018), p. 471-476.doi:<https://doi.org/10.15407/fm25.03.471>

© 2018 — STC "Institute for Single Crystals"

## Interaction of $\text{HNO}_3$ –HI-citric acid aqueous solutions with $\text{CdTe}$ , $\text{Zn}_{0.04}\text{Cd}_{0.96}\text{Te}$ , $\text{Zn}_{0.1}\text{Cd}_{0.9}\text{Te}$ and $\text{Cd}_{0.2}\text{Hg}_{0.8}\text{Te}$ semiconductors

*Ye.Ye.Hvozdiyevskiy<sup>1</sup>, R.O.Denysyuk<sup>1</sup>, V.M.Tomashyk<sup>2</sup>,  
G.P.Malanych<sup>2</sup>, Z.F.Tomashyk<sup>2</sup>*

<sup>1</sup>I.Franko Zhytomyr State University,

40 Velyka Berdychivska Str., 10008 Zhytomyr, Ukraine

<sup>2</sup>V.Lashkaryov Institute of Semiconductor Physics, National Academy of Sciences of Ukraine, 41 Nauki Ave., 03028 Kyiv, Ukraine

*Received January 25, 2018*

The chemical dissolution of  $\text{CdTe}$  single crystals and  $\text{Zn}_{0.04}\text{Cd}_{0.96}\text{Te}$ ,  $\text{Zn}_{0.1}\text{Cd}_{0.9}\text{Te}$ ,  $\text{Cd}_{0.2}\text{Hg}_{0.8}\text{Te}$  solid solutions in  $\text{HNO}_3$ –HI-citric acid aqueous solutions has been investigated. The etching rate dependences of the mentioned above materials versus iodine and organic solvent content in the compositions of the chemical dissolution have been determined. The projections of constant etch rate surfaces (the Gibbs diagrams) have been constructed, the kinetic features of the dissolution has been shown and rate-limiting steps of the dissolution process and locate composition regions of polishing solutions have been identified. Using the experimental data, the compositions of polishing solutions and the conditions of the chemical-dynamic polishing of the  $\text{CdTe}$ ,  $\text{Zn}_{0.04}\text{Cd}_{0.96}\text{Te}$ ,  $\text{Zn}_{0.1}\text{Cd}_{0.9}\text{Te}$  and  $\text{Cd}_{0.2}\text{Hg}_{0.8}\text{Te}$  surfaces have been optimized.

**Keywords:** semiconductor, single crystal, solid solutions, etchant, surface, chemical etching, polishing, kinetics.

Исследованы процессы химического растворения монокристаллов  $\text{CdTe}$  и твердых растворов  $\text{Zn}_{0.04}\text{Cd}_{0.96}\text{Te}$ ,  $\text{Zn}_{0.1}\text{Cd}_{0.9}\text{Te}$  и  $\text{Cd}_{0.2}\text{Hg}_{0.8}\text{Te}$  в водных растворах  $\text{HNO}_3$ –HI-лимонная кислота. Определены зависимости скорости травления указанных материалов от концентрации окислителя и органического растворителя. Построены поверхности одинаковых скоростей травления (диаграммы Гиббса), установлены кинетические закономерности и определены лимитирующие стадии процесса растворения и области полирующих растворов. Оптимизированы составы полирующих травителей и режимы химико-динамического полирования поверхности исследуемых полупроводниковых материалов.

**Взаємодія водних розчинів  $\text{HNO}_3$ –HI-цитратна кислота з напівпровідниками  $\text{CdTe}$ ,  $\text{Zn}_{0.04}\text{Cd}_{0.96}\text{Te}$ ,  $\text{Zn}_{0.1}\text{Cd}_{0.9}\text{Te}$  та  $\text{Cd}_{0.2}\text{Hg}_{0.8}\text{Te}$ . Є.Є.Гвоздієвський, Р.О.Денисюк, В.М.Томашик, Г.П.Маланич, З.Ф.Томашик.**

Досліджено процеси хімічного розчинення монокристалів  $\text{CdTe}$  та твердих розчинів  $\text{Zn}_{0.04}\text{Cd}_{0.96}\text{Te}$ ,  $\text{Zn}_{0.1}\text{Cd}_{0.9}\text{Te}$  і  $\text{Cd}_{0.2}\text{Hg}_{0.8}\text{Te}$  у водних розчинах  $\text{HNO}_3$ –HI-цитратна кислота. Визначено залежності швидкості травлення вказаних матеріалів від концентрації окисника та органічного розчинника. Побудовано поверхні однакових швидкостей травлення (діаграми Гіббса), встановлено кінетичні закономірності та визначено лімітуючі стадії процесу розчинення і області поліруючих розчинів. Оптимізовано склади поліруючих травників і режими хіміко-динамічного полірування поверхні напівпровідникових матеріалів, що досліджувалися.

## 1. Introduction

II–VI semiconductors, in particular, cadmium telluride and  $\text{Zn}_x\text{Cd}_{1-x}\text{Te}$ ,  $\text{Cd}_x\text{Hg}_{1-x}\text{Te}$  solid solutions are widely used for manufacturing of the modern electronics devices. The wide-band gap semiconductor crystals of  $\text{Zn}_x\text{Cd}_{1-x}\text{Te}$  ( $x = 0.04$  to  $0.1$ ) solid solutions are promising materials for the manufacture of working elements of X-ray and  $\gamma$ -radiation detectors and the  $\text{Cd}_x\text{Hg}_{1-x}\text{Te}$  solid solutions are key materials in fabrication of IR-photodetectors [1, 2].

Semiconductor materials intended for the formation of electronics devices must be perfect concerning the atomic structure and have a perfect surface. Therefore, it is necessary to carry out research of the processes that occur at the surface of the mentioned above semiconductors with various active solutions in order to create the new etching compositions and modes of surface modification of the II–VI semiconductor materials. For obtaining the high-quality polishing and structurally perfect surfaces of the CdTe and  $\text{Zn}_x\text{Cd}_{1-x}\text{Te}$  and  $\text{Cd}_x\text{Hg}_{1-x}\text{Te}$  solid solutions, with simultaneous retaining the needed geometrical parameters, chemical-dynamic polishing (CDP) and chemical-mechanical polishing are used. Chemical etching based on chemical dissolution processes is one of the main technological operations in the chemical treatment of semiconductor single crystals, which are widely used in manufacturing of different semiconductor devices and integrated circuits [3]. Surface processing usually includes two steps: (1) mechanical polishing that diminishes the damage on the crystal's surfaces after cutting, and (2) chemical etching that removes a certain amount of material from the top layers of the surfaces, thus leaving behind a comparatively smooth surface depending on the extent of damage caused mechanical polishing.

Among the widely used etchants, the solutions of bromine in methanol are the most popular for treatment of the CdTe,  $\text{Zn}_x\text{Cd}_{1-x}\text{Te}$  and  $\text{Cd}_x\text{Hg}_{1-x}\text{Te}$  surfaces [4, 5]. However, after the treatment with such solutions the surface is enriched with Te which is easily oxidized on exposure in air. In addition, employing bromine-based etchants generates some features on treated surfaces, and can leave behind some residues after chemical polishing [6].

Denysyuk et al. [7] investigated the chemical etching processing of the CdTe and  $\text{Zn}_{0.04}\text{Cd}_{0.96}\text{Te}$ ,  $\text{Zn}_{0.1}\text{Cd}_{0.9}\text{Te}$  and

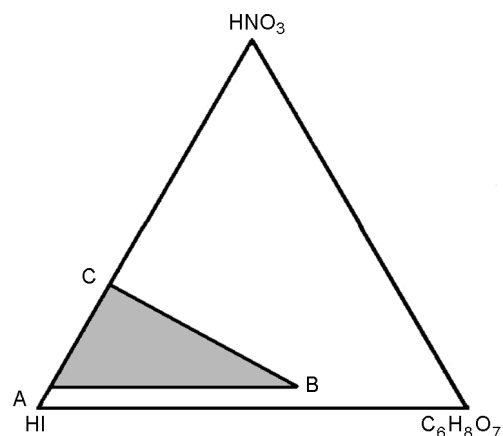


Fig. 1. Investigated concentration range of  $\text{HNO}_3 + \text{HI} + \text{C}_6\text{H}_8\text{O}_7$  solutions at volume ratio of component  $\text{HNO}_3$  (70 mass. %):HI (54 mass. %):citric acid (20 mass. %) at vertices A, B, C, respectively: A — 5:95:0; B — 5:35:60; C — 25:75:0.

$\text{Cd}_{0.2}\text{Hg}_{0.8}\text{Te}$  solid solutions single crystals with  $\text{I}_2$  in HI solutions. The dissolution rate of the semiconductor materials increases from  $5.0$  to  $14.3 \mu\text{m}/\text{min}$ , at the iodine concentration changing in the etching composition from 3 to 15 mass. %. At the concentration value of 3 mass. % of  $\text{I}_2$  in the HI solution, the CdTe surface is covered with a thin oxide layer.

Chemical treatment of the CdTe and  $\text{Zn}_x\text{Cd}_{1-x}\text{Te}$  solid solutions was spent using etchant containing  $\text{HNO}_3$ -HI-tartratic acid ( $\text{C}_4\text{H}_6\text{O}_6$ ) solutions [8]. Comparing the results of chemical etching of CdTe and  $\text{Zn}_x\text{Cd}_{1-x}\text{Te}$  with the  $\text{HNO}_3$ -HCl- $\text{C}_4\text{H}_6\text{O}_6$  (Cl, Br) solutions it was determined that not only the concentration region of polishing solutions, but also the dissolution rate of the material as well as the quality of the polished surface have been changed [8, 9]. The etching rate of the crystals decreases and the quality of polishing surfaces improves at the using in the etchant compositions HI instead of HCl or HBr. The addition of an organic acid to etchant compositions improves their polishing performance.

The objective of this work is to study the chemical etching of  $\text{Zn}_{0.04}\text{Cd}_{0.96}\text{Te}$ ,  $\text{Zn}_{0.1}\text{Cd}_{0.9}\text{Te}$  and  $\text{Cd}_{0.2}\text{Hg}_{0.8}\text{Te}$  solid solution and CdTe single crystals with  $\text{HNO}_3$ -HI- $\text{C}_6\text{H}_8\text{O}_7$  (citric acid) iodine-emerging solutions, and to develop and optimize the etchant compositions and choice of technological modes to form the structurally perfect quality defectless surface.

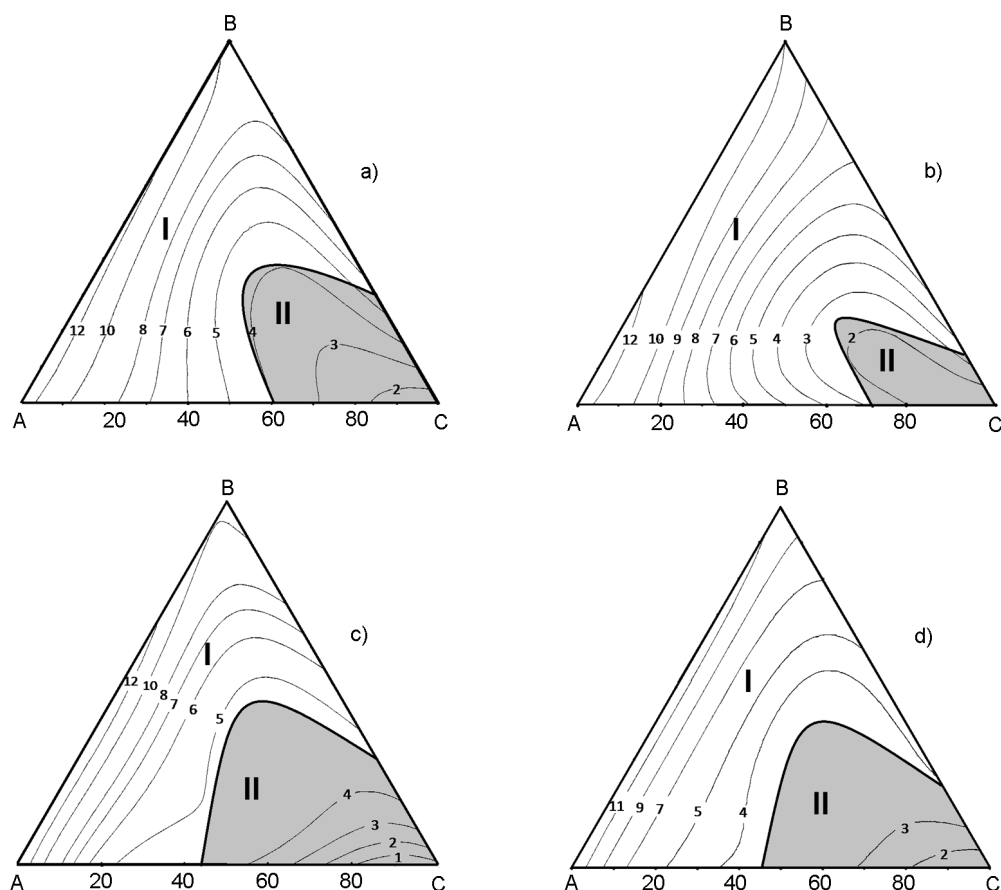
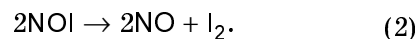


Fig. 2. Etch rate ( $\mu\text{m}/\text{min}$ ) versus etchant composition diagrams ( $T = 293\text{ K}$ ,  $\gamma = 82\text{ rpm}$ ) for (a) CdTe, (b)  $\text{Zn}_{0.04}\text{Cd}_{0.96}\text{Te}$ , (c)  $\text{Zn}_{0.1}\text{Cd}_{0.9}\text{Te}$ , and (d)  $\text{Cd}_{0.2}\text{Hg}_{0.8}\text{Te}$  in  $\text{HNO}_3$ -HI-citric acid solutions; the  $\text{HNO}_3$ :HI: $\text{C}_6\text{H}_8\text{O}_7$  volume ratio in corners A, B, and C is 5:95:0, 5:35:60, and 25:75:0, respectively; (I) polishing and (II) nonpolishing solutions.

## 2. Experimental

In our experiments, we used Bridgman-grown  $n$ -type single crystals of undoped CdTe and  $\text{Zn}_{0.04}\text{Cd}_{0.96}\text{Te}$ ,  $\text{Zn}_{0.1}\text{Cd}_{0.9}\text{Te}$  and  $\text{Cd}_{0.2}\text{Hg}_{0.8}\text{Te}$  solid solutions. Samples with  $\approx 0.5\text{ cm}^2$  in area and 1.5–2 mm in thickness were cut from the single-crystalline ingots by a diamond wire saw lubricated with distilled water during the cutting process. After mechanical polishing, the samples were glued with picein by their non-working side to quartz substrates and placed into the sample holder of a CDP setup in which dissolution was carried out in the rotating disk mode. Before dissolution kinetic experiments, a layer of 100–150  $\mu\text{m}$  thick, damaged by preceding mechanical treatment, was removed from the surface by the chemical-mechanical polishing in the solution to be studied. We dissolved three or four samples simultaneously. Limiting stages of the materials dissolution process were deter-

mined by studying the etching rate dependencies on the solution temperature ( $T = 283\text{--}303\text{ K}$ ) and disk rotation speed ( $\gamma = 22\text{--}122\text{ rpm}$ ). The etchants were prepared from 54 Wt % HI, 70 Wt %  $\text{HNO}_3$  and 20 Wt % citric acid ( $\text{C}_6\text{H}_8\text{O}_7$ ); aqueous solutions of sodium thiosulfate were used for post-treatment cleaning. All chemicals were of chemically pure grade. After the preparation, the solutions were left to stand for 2 h to reach equilibrium. In  $\text{HNO}_3 + \text{HI}$  mixtures, the constituent components of  $\text{HNO}_3$  and HI react to give elemental iodine, forming so-called iodine-emerging solutions:



After the chemical-dynamic polishing, the samples were washed in aqueous solutions of 0.2 M  $\text{Na}_2\text{S}_2\text{O}_3$  and several times in

Table 1. Apparent activation energy ( $E_a$ ) for the diffusion-limited dissolution of semiconductor in a solution with the composition (vol. %)  $10\text{HNO}_3 + 75\text{HI} + 15\text{C}_6\text{H}_8\text{O}_7$  ( $\gamma = 82$  rpm)

Semiconductor	CdTe	$\text{Zn}_{0.04}\text{Cd}_{0.96}\text{Te}$	$\text{Zn}_{0.1}\text{Cd}_{0.9}\text{Te}$	$\text{Cd}_{0.2}\text{Hg}_{0.8}\text{Te}$
$E_a$ , $\text{kJ}\cdot\text{mol}^{-1}$	27.83	21.11	12.37	14.58

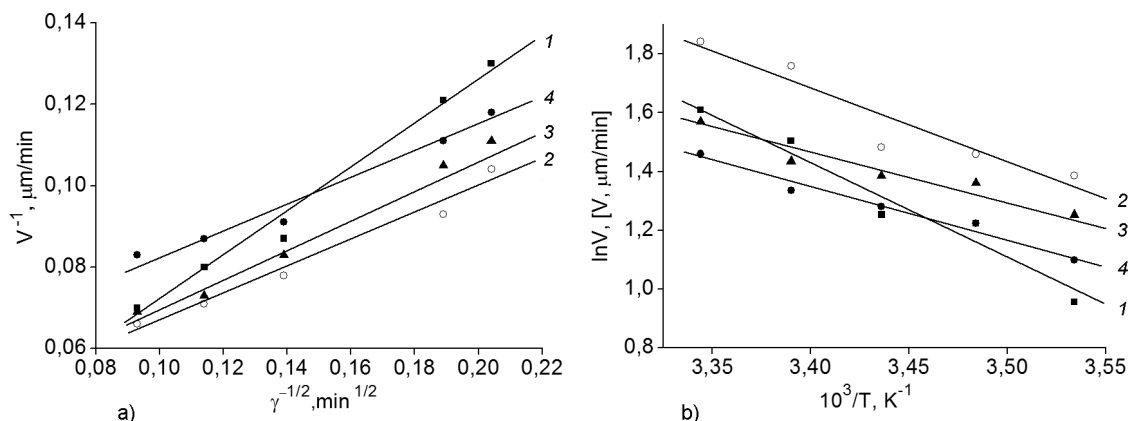
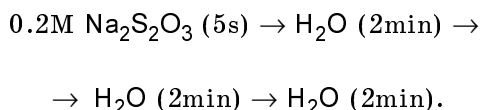


Fig. 3. Dissolution rate as a function of (a) etchant stirring rate ( $T = 293$  K) and (b) temperature ( $\gamma = 82$  rpm) for CdTe (1),  $\text{Zn}_{0.04}\text{Cd}_{0.96}\text{Te}$  (2),  $\text{Zn}_{0.1}\text{Cd}_{0.9}\text{Te}$  (3) and  $\text{Cd}_{0.2}\text{Hg}_{0.8}\text{Te}$  (4) in a solution with the composition (vol. %)  $10\text{HNO}_3 + 75\text{HI} + 15\text{C}_6\text{H}_8\text{O}_7$ .

distilled water according to the following scheme:



Next, the samples were dried in flowing dry air. After the chemical treatment, the investigated samples must be storage in dimethylformamide or isopropanol solution, where the polished surface doesn't lose its properties during several months.

The dissolution rate was determined by the wafer thickness reduction using a 1 MIGP time indicator to within  $\pm 0.5$   $\mu\text{m}$ , and deviations in the measured thickness did not exceed 5 %.

Microstructure of the etched surfaces was examined with a Zeiss Jenatech Inspection microscope equipped with a digital video camera with the magnifications from  $\times 25$  to  $\times 1600$ . To inspect the micro-relief and surface structure of the etched wafers, the surface roughness was determined by a mechanical contact method. Measurements were carried out on a HOMMEL-ETAMIC W5 profilometer, which allows determining the heights of the surface's profile  $\geq 5$  nm.

The morphology of the polished surfaces of the single crystals of the CdTe and  $\text{Zn}_{0.04}\text{Cd}_{0.96}\text{Te}$ ,  $\text{Zn}_{0.1}\text{Cd}_{0.9}\text{Te}$  and  $\text{Cd}_{0.2}\text{Hg}_{0.8}\text{Te}$  solid solutions was examined by atomic force microscopy (AFM). In the

former instance, we used tapping mode imaging on a NanoScope IIIa Dimension 3000 scanning probe microscope (Digital Instruments/Brukes Corp.) under ambient conditions with commercial NCH silicon cantilever probes (Nano World, nominal probe tip radius of down to 10 nm).

### 3. Results and discussion

For our investigation, we chose experimentally the solution concentrations in composition triangle ABC which is given in Fig. 1. The solutions concentration interval was selected taking into account the necessity to avoid the passivation areas and two-phase solutions.

Fig. 2 shows the dependence of the CdTe,  $\text{Zn}_{0.04}\text{Cd}_{0.96}\text{Te}$ ,  $\text{Zn}_{0.1}\text{Cd}_{0.9}\text{Te}$  and  $\text{Cd}_{0.2}\text{Hg}_{0.8}\text{Te}$  etching rates on the composition of aqueous  $\text{HNO}_3$ –HI–citric acid solutions ( $T = 293$  K and disc rotation speed  $\gamma = 82$  rpm), constructed using the mathematical simulation of the experiment on the simplex. Analysis of the Gibbs diagrams leads us to conclude that the etching of all samples occurs by the same mechanism, as evidenced by the fact that the iso-lines of dissolution rate are similar in shape. The process of dissolution plates in the mixtures is characterized by slow etching rates (1.0–12.0  $\mu\text{m}/\text{min}$ ). The dissolution rate of the semiconductor in the  $\text{HNO}_3$ –HI– $\text{C}_6\text{H}_8\text{O}_7$  solutions has a maximum in mixtures enriched in iodide acid (corner A in

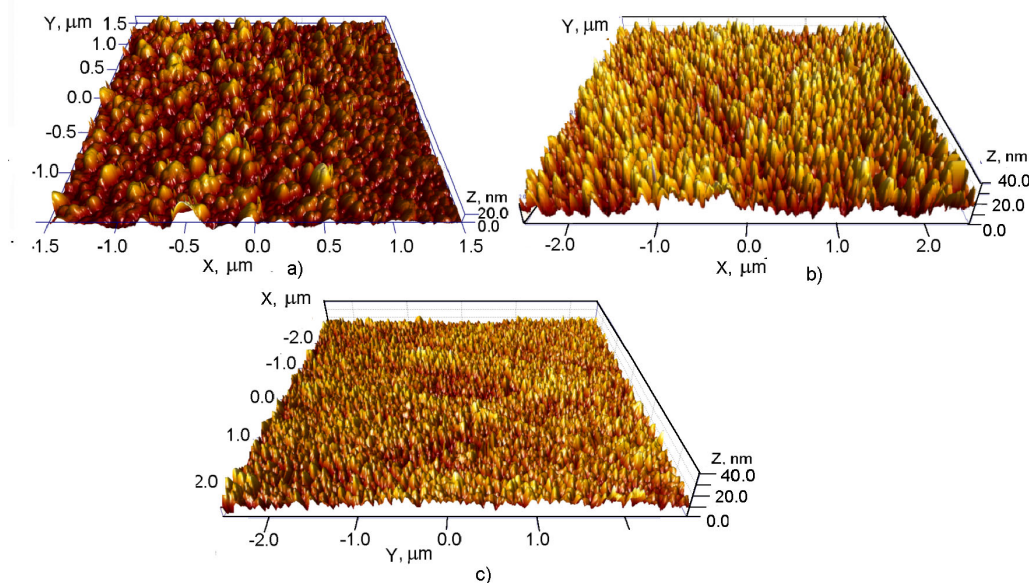


Fig.4 Three-dimensional AFM images of the CdTe surface after CMP with a  $\text{HNO}_3$  – HI – EG (a), CDP with the same etchant (b) and CDP with a  $\text{HNO}_3$  – HI – citric acid (c) (the etching was conducted with a polishing solutions; CMP: 2 min,  $T = 293$  K; CDP: 5 min,  $T = 293$  K,  $\gamma = 82$  rpm).

the triangles) and a minimum in the mixtures enriched in citric acid (at 60 vol. %  $\text{C}_6\text{H}_8\text{O}_7$ , corner C). With a content of  $\text{C}_6\text{H}_8\text{O}_7$  over 40 vol. % passivation of the surface occurs, which is accompanied by the formation of a gray deposit.

To assess the kinetics and identify the rate-controlling steps of the dissolution of CdTe,  $\text{Zn}_{0.04}\text{Cd}_{0.96}\text{Te}$ ,  $\text{Zn}_{0.1}\text{Cd}_{0.9}\text{Te}$  and  $\text{Cd}_{0.2}\text{Hg}_{0.8}\text{Te}$ , we examined the dissolution rate ( $v$ ) as a function of temperature and disk rotation speed ( $\gamma$ ) in polishing solution with the composition (vol. %)  $10\text{HNO}_3 + 75\text{HI} + 15\text{C}_6\text{H}_8\text{O}_7$ . The dissolution rate versus disk rotation speed were represented as plots of  $v^{-1}$  against  $\gamma^{-1/2}$  at  $\gamma = 22$ –122 rpm ( $T = 293$  K), and the temperature-dependent dissolution rate data in the range of 283–303 K ( $\gamma = 82$  rpm) were represented as plots of  $\ln v$  against  $1/T$  (Fig. 3).

The corresponding lines for the CdTe (1),  $\text{Zn}_{0.04}\text{Cd}_{0.96}\text{Te}$  (2),  $\text{Zn}_{0.1}\text{Cd}_{0.9}\text{Te}$  (3) and  $\text{Cd}_{0.2}\text{Hg}_{0.8}\text{Te}$  (4) crystals (Fig. 3a, curves 1–4) could be extrapolated to the origin, suggesting that the dissolution process is diffusion-controlled.

From the temperature dependences of the etching rate (Fig. 3b) the values of apparent activation energy ( $E_a$ ) were calculated for all crystals using the Arrhenius equation ( $v = C_E \cdot e^{-E_a/RT}$ ). The calculated apparent activation energy was found to be no higher than 35 kJ/mol (see Table 1),

which is characteristic of the diffusion-limited dissolution processes [10].

Table 2 summarizes the main surface roughness parameters  $R_a$ ,  $R_z$ , and  $R_{max}$  of the CdTe wafers after cutting and subsequent grinding. The measurements were performed over a base length of 0.25 mm at a tracing length of 1.5 mm.

Using AFM, we obtained the data on the surface structure for all samples under investigation after CMP and DCP. Figure 4 illustrates the image of the CdTe surfaces after CMP (Fig. 4a) and CDP (Fig. 4b). After CMP with the new  $\text{HNO}_3$ –HI–ethylene glycol etchant mixtures, the surface of the crystals had the following surface roughness parameters: arithmetic mean surface roughness ( $R_a$ ) for CdTe – 6.8 nm,  $\text{Zn}_{0.04}\text{Cd}_{0.96}\text{Te}$  – 5.3 nm, and  $\text{Cd}_{0.2}\text{Hg}_{0.8}\text{Te}$  – 1.5 nm (the analyzed area is  $3 \times 3$ ). After the next stage of processing by the method of CDP using the  $\text{HNO}_3$ –HI–citric acid polishing composition, the values of  $R_a$  are somewhat higher, but  $R_a < 10$  nm. One possible reason for this is that during the CMP process, the sample surface experiences the combined effect of etchant and soft polisher, which helps to ensure uniform etching throughout the sample surface and eliminate all of the irregularities.

It should be noted that for the super-smooth polished surfaces of semiconductor materials, the value of  $R_a$  should not exceed 10 nm [11].

Table 2. CdTe surface roughness parameters obtained with a HOMMEL-ETAMIC W5 profilometer after various machining stages

Machining stages	$R_a$ , $\mu\text{m}$	$R_z$ , $\mu\text{m}$	$R_{\text{max}}$ , $\mu\text{m}$	Surface condition*
wire saw cutting	1.2	6.0	7.9	wavy, rough surface with cutting traces (longitudinal scratches)
wire saw cutting + grinding with free M10 abrasive	0.5	2.8	3.7	dull, rough surface with structural defects
wire saw cutting + grinding with free M10 + M5 abrasive	0.2	1.3	1.6	dull, rough surface with structural defects

$R_a$  is the arithmetic mean of the profile height within a base length,  $R_z$  is the sum of the average magnitudes of the five highest elevations and the depths of the five lower valleys in the surface profile, and  $R_{\text{max}}$  is the maximum profile height.

\* MIM-7 with an eTREK DCM800 digital video camera (8 Mpix).

Summarizing the obtained results on the surface morphology of the CdTe,  $\text{Zn}_{0.04}\text{Cd}_{0.96}\text{Te}$ ,  $\text{Zn}_{0.1}\text{Cd}_{0.9}\text{Te}$ , and  $\text{Cd}_{0.2}\text{Hg}_{0.8}\text{Te}$  crystals, one can state the possibility of using the  $\text{HNO}_3$ -HI- $\text{C}_6\text{H}_8\text{O}_7$  polishing solutions to obtain a high-quality polished surface of the above-mentioned semiconductors using chemical-dynamic polishing.

#### 4. Conclusion

We have studied the chemical dissolution of CdTe,  $\text{Zn}_{0.04}\text{Cd}_{0.96}\text{Te}$ ,  $\text{Zn}_{0.1}\text{Cd}_{0.9}\text{Te}$  and  $\text{Cd}_{0.2}\text{Hg}_{0.8}\text{Te}$  semiconductors in  $\text{HNO}_3$ -HI-citric acid iodine-emerging etchants. The "dissolution rate-etchant composition" diagrams have been constructed, the composition regions of polishing solutions have been determined, and the compositions of polishing  $\text{HNO}_3$ -HI-citric acid etchants and CDP conditions have been optimized. Using the dependences of the dissolution rate versus temperature and disk rotation speed, the dissolution of the materials under study in  $\text{HNO}_3$ -HI-citric acid polishing solutions has been shown to be diffusion-limited.

#### References

- Ye.O.Bilevych, V.M.Tomashik, Z.F.Tomashik, S.G.Danylenko, *Phys.Chem.Solid State*, **1**, 267 (2000).
- Z.F.Tomashik, O.R.Gumenyuk, V.N.Tomashik, P.I.Feychuk, *Kondens.Sredy i Mezhfaz.Granitsy*, **5**, 248 (2003).
- V.N.Tomashik, Z.F.Tomashik. in: CdTe and Related Compounds; Physics, Defects, Hetero- and Nano-Structures, Crystal Growth, Surfaces and Applications. P.II. ed. by R.Triboulet and P.Siffert, Netherlands (2010).
- R.R. Singh, D. Kaushik, M. Sharma, D.K. Gupta, R.K. Pandey. *Semicond. Sci. Technol*, **23**, 015016 (2008).
- L. Qiang, J. Wanqi., *Semicond. Sci. Technol.*, **21**, 72, (2006).
- A. Hossain, A.E. Bolotnikov, G.S. Camarda, et.al., *J. Electron. Mater.*, **43**, 2771, (2014).
- R.O.Denysyuk, V.M.Tomashik, E.E.Hvozdiyevskiy, *Vopr.Khim.Khim.Tekhnol.*, **2**, 51 (2016).
- Z.F.Tomashik, Ye.O.Bilevych, V.N.Tomashik, *Kondens.Sredy i Mezhfaz.Granitsy*, **3**, 237 (2001).
- Z.F. Tomashik, Ye.O. Bilevych, V.N. Tomashik, *Kondens. Sredy i Mezhfaz. Granitsy*, **3**, 237 (2001).
- E.E.Hvozdiyevskiy, R.O.Denysyuk, V.M.Tomashik et al., *Nauk.Visn.Chernivtsi Nats.Univ.Khim.*, **658**, 136 (2013).
- V.A.Perevoshchikov, *Vysokochistye Veshchestva*, **2**, 5 (1995).
- S.S. Pop, I.S. Sharodi, Physical Electronics, Lviv, Yevrosvit (2001) [in Ukrainian].